

Featuring work from Professor Yanwei Jia's laboratory,
State Key Laboratory of Analog and Mixed-Signal VLSI,
Institute of Microelectronics, University of Macau,
Macau, China.

Clip-to-release on amplification (CRoA): a novel DNA
amplification enhancer on and off microfluidics

“Clip-to-release on amplification” mechanism clips
dsDNA-binding dyes and releases them on demand during
DNA amplification. This simple but effective strategy would
reignite the utilization of dsDNA dyes for a wider application
in DNA analysis both on-chip and off-chip.

As featured in:



See Yanwei Jia *et al.*,
Lab Chip, 2020, **20**, 1928.


 Cite this: *Lab Chip*, 2020, 20, 1928

Clip-to-release on amplification (CRoA): a novel DNA amplification enhancer on and off microfluidics†

 Ren Shen, ^{ab} Yanwei Jia, ^{*abc} Pui-In Mak^{ab} and Rui P. Martins^{abd}

Despite its high sensitivity, low cost, and high efficiency as a DNA amplification indicator with a yes/no answer, dsDNA-binding dye encounters incompatibility when used in microfluidic systems, resulting in problems such as false negative amplification results. Besides, its inhibition of amplification at high concentrations hinders its application both on-chip and off-chip. In this study, we propose a novel DNA amplification enhancer to counteract the drawbacks of dsDNA-binding dyes. It acts as a temporary reservoir for the free-floating dyes in solution and releases them on demand during the amplification process. Through this clip-to-release on amplification mechanism, the enhancer lowered the background fluorescence of sample droplets before amplification, enhanced the signal-to-background ratio of positive samples, and eliminated the false negative signal of on-chip PCR. Moreover, the enhancer increased the off-chip polymerase chain reaction (PCR) efficiency, boosted the fluorescence signal up to 10-fold, and made less nonspecific amplification product. All the factors affecting the enhancer's performance are investigated in detail, including its structure and concentration, and the types of dsDNA-binding dye used in the reaction. Finally, we demonstrated the broad application of the proposed amplification enhancer in various DNA amplification systems, for various genes, and on various amplification platforms. It would reignite the utilization of dsDNA dyes for wider applications in DNA analysis both on-chip and off-chip.

 Received 29th March 2020,
 Accepted 22nd April 2020

DOI: 10.1039/d0lc00318b

rsc.li/loc

Introduction

Nucleic acid amplification methods such as polymerase chain reaction (PCR) and loop-mediated isothermal amplification (LAMP) are powerful molecular biology tools used in various areas such as basic biology research, clinical diagnosis, and inspection and quarantine. To detect the DNA amplification products in a closed-tube system, either in real-time or through post-amplification analysis such as melting curve analysis, fluorogenic reporters are added into the reaction mixture.¹ These reporters mainly fall into two groups: one group is specific DNA probes which are often labeled with fluorophores,² and the other group is dsDNA-binding dyes, such as EtBr,³ SYBR Green I (SGI),⁴ EvaGreen,⁵ and Sytox Green.⁶ The probe-based reporting system is specific and applicable to multiplex detection by utilizing different fluorophores. However, the cost of synthesizing these dual-

labeled probes is high, and the design or optimization of specific probes for different target sequences is time-consuming. Besides, probes have various limitations based on their type. For example, for Taqman probes,^{7,8} the high T_m requirement for a probe adds limitations to the probe design; for molecular beacon (MB) probes,^{9,10} single-stranded DNA amplicons are needed to bind with the probe.

Compared to specific probes, dsDNA-binding dyes cost much less per reaction.¹¹ These dyes bind with dsDNA nonspecifically, either by intercalating or through a minor groove binding mechanism.^{12–14} Upon binding, the dyes emit much stronger fluorescence than when they are free in solution, making them highly sensitive to dsDNA amplicons. Amplification specificity can be achieved by careful primer design. Therefore, for a quick yes/no answer for a certain target, dsDNA dye is a sensitive, bright and low-cost option.

Despite their excellent performance, the application of dsDNA-binding dyes in PCR and related techniques is limited by their incompatibility with microfluidic systems, as well as their inhibition of amplification efficiency at high concentrations, especially in the case of SGI.¹¹ In recent years, because of microfluidic devices' low reagent consumption, short reaction time, and miniaturized device setting, the integration of nucleic acid amplification methods with microfluidic systems has been a focus of research.^{15–17} This

^a State-Key Laboratory of Analog and Mixed-Signal VLSI, Institute of Microelectronics, University of Macau, Macau, China.

E-mail: yanweijia@um.edu.mo; Tel: +853 88224451

^b Faculty of Science and Technology – ECE, University of Macau, Macau, China

^c Faculty of Health Sciences, University of Macau, Macau, China

^d On Leave from Instituto Superior Técnico, Universidade de Lisboa, Portugal

† Electronic supplementary information (ESI) available. See DOI: 10.1039/d0lc00318b

technical convergence has resulted in a big step forward towards the lab-on-a-chip system.^{18–23} However, we noticed that dsDNA-binding dyes such as SGI often failed to function well as an amplification indicator on-chip, sometimes presenting false negative results on both digital microfluidic and PDMS-based channel microfluidic devices. The dye had difficulty lighting up after PCR with positive samples, even when the amplification products were confirmed by gel electrophoresis. Besides this severe functional failure we observed, dsDNA binding dyes were reported to have poor performance in some on-chip applications. For example, Di Carlo's group²⁴ found that EvaGreen generated too weak fluorescence signals in their hand-held LAMP system. Besides, Houssin's group¹⁸ encountered a delayed Cq when SGI was applied in a real-time on-chip amplification assay, compared with the corresponding off-chip assay. The dsDNA dyes' poor on-chip performance may be due to the adsorption of reagents on the surfaces of the microfluidic chips,^{14,25} the diffusion of reagents into surrounding oil, the photobleaching effect of the dye,^{26,27} or other factors. Whatever issues cause this problem, the incompatibility of dsDNA dyes with microfluidic devices hinders research progress and applications focused on on-chip nucleic acid analysis.

To counteract the drawbacks of dsDNA-binding dyes and better utilize them in both on-chip and off-chip scenarios, other researchers have proposed some PCR enhancers to target these dyes. For example, Di Carlo's group²⁴ found that HNB interacted with EvaGreen to lower the background intensity as well as increase the amplification efficiency. Dráber's group²⁸ proposed that tetraalkylammonium derivatives enhanced SGI-monitored real-time PCR by reducing SGI's binding with primers. Besides, magnesium

chloride was found by Nath *et al.*²⁹ to be able to partially reverse the inhibitory effects of EtBr and SGI on PCR. However, these additives functioned in an ion-dependent manner and their enhancing effect could only be modulated by changing their concentration, thus in a limited range.

In this study we propose a novel nucleic acid amplification enhancer with a clip-to-release on amplification mechanism, and name it CRoA. As illustrated in Fig. 1, the proposed enhancer is a hairpin-structured oligonucleotide with a 3' quencher, where the double-stranded stem acts as a reservoir and shelter for dye molecules and the quencher quenches out the fluorescence from the stocked dye. Since dsDNA-binding dyes such as SGI tend to bind preferentially to larger amplicons,³⁰ as amplification proceeds the dye molecules can hop from the temporary stem reservoir to longer target amplicons. Experimental results show that the CRoA enhancer can not only restore and enhance the dyes' signal for on-chip PCR, but also increase the amplification efficiency at a high dye concentration. Thus, the proposed CRoA enhancer can broaden the dynamic range of dsDNA-binding dyes, as well as improve the amplification performance and reliability of the results in both on-chip and off-chip amplification systems. (Detailed description of materials and methods used in this study can be found in the ESI.†)

Results and discussion

Proof-of-principle of CRoA enhancing effect

SGI at a high concentration causes inhibition of PCR, as Fig. 2A reveals. In the G269 symmetric PCR system, compared to 0.4× SGI, doubling the concentration to 0.8×

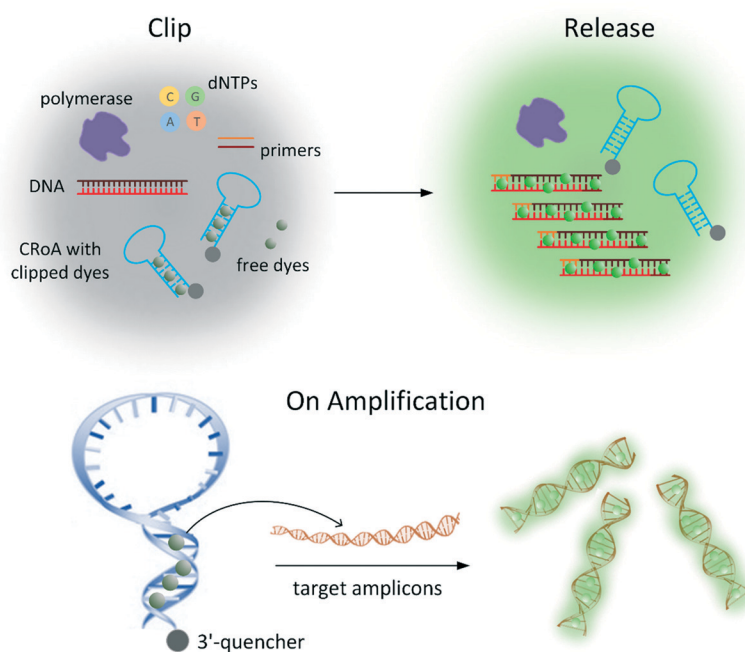


Fig. 1 Schematic of CRoA (clip-to-release on amplification) mechanism as an amplification enhancer (the dye molecules in the figure do not indicate the exact number of dye molecules clipped by dsDNA).

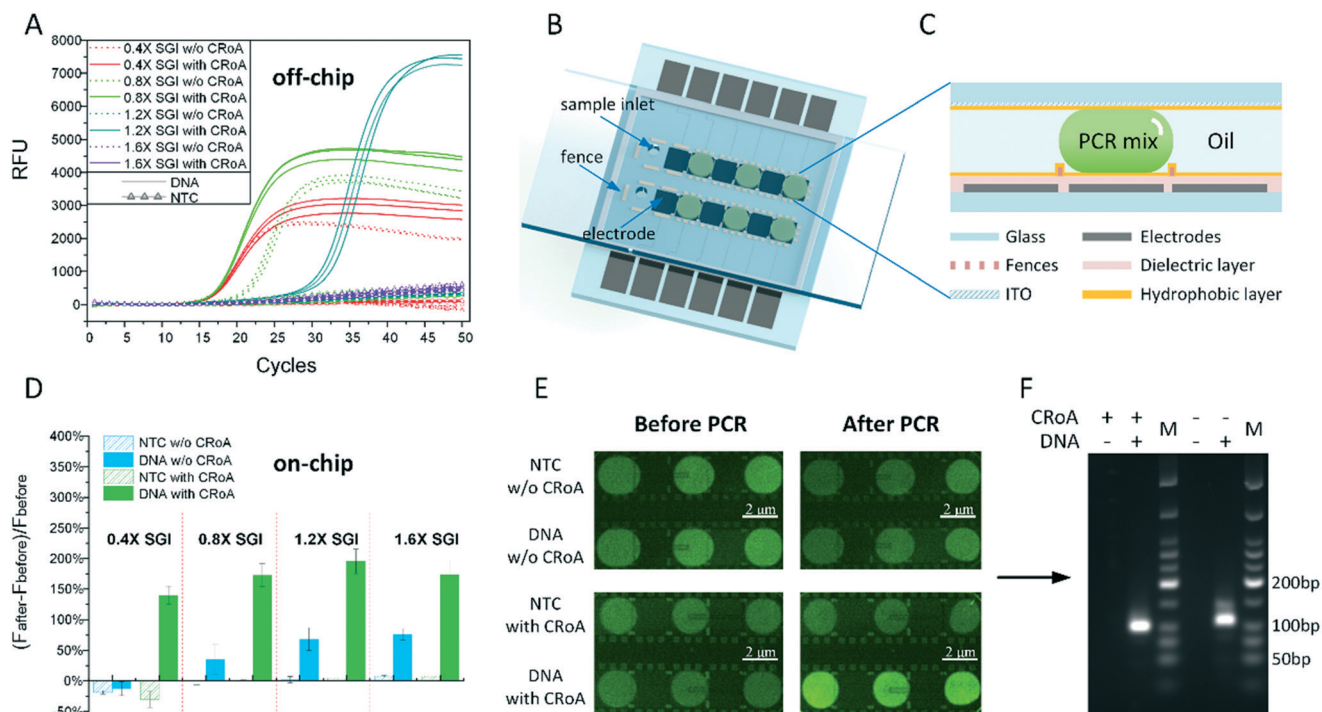


Fig. 2 Proof of principle experiments of the CRoA PCR enhancing function for off-chip and on-chip PCR. The CRoA enhancer used here was A4Q in Table S1,† at 500 nM concentration in the reaction mixture. (A) Off-chip amplification curves compared between samples with and w/o the CRoA enhancer, at 0.4 \times , 0.8 \times , 1.2 \times , and 1.6 \times SGI. (B and C) Top view and side view schematics of the DMF chip used. (D) End-point analysis results of on-chip PCR compared between samples with and w/o the CRoA enhancer, at 0.4 \times , 0.8 \times , 1.2 \times , and 1.6 \times SGI. (E) Fluorescence images of samples before and after on-chip PCR at 0.4 \times SGI. (F) Gel electrophoresis result of on-chip PCR products at 0.4 \times SGI. Each lane included the triplicate droplets shown in Fig. 2E. M represents the DNA ladder.

delayed the C_q value for 3 cycles. Further increasing the concentration to 1.2 \times resulted in a failed PCR. By adding CRoA to the PCR reaction mixture, this inhibition was reduced. With CRoA, 0.8 \times SGI caused no inhibition, and the templates were successfully amplified at 1.2 \times SGI, though with a C_q delay. This result can be attributed to the structure of CRoA. Since SGI has a high affinity to dsDNA,³⁰ the double-stranded stem in the CRoA hairpin structure offers a temporary reservoir for the dye molecules. Instead of being free in the solution, a large number of SGI molecules are clipped by the stem of CRoA, causing less interference to the amplification process. As amplification goes on, the newly produced amplicons with a larger size than the CRoA stem become a better choice for SGI, due to the dye's preference for longer dsDNA strands. *Via* this mechanism, SGI's interference with the polymerase and other functioning reagents is reduced, while its function as an amplification indicator is maintained.

The function of CRoA in on-chip PCR was investigated with a digital microfluidic (DMF) system. The schematic setup of the DMF system is shown in Fig. 2B and C. Detailed fabrication and operation processes, system setup (Fig. S1†), and normalization method for on-chip fluorescence data (Fig. S2†) can be found in the ESI.†

As displayed in Fig. 2D, in the absence of CRoA, the SGI signal was weakened after thermal cycling on the DMF chip.

This greatly attenuated the reliability of the end-point analysis of on-chip PCR which used SGI as the indicator. Especially at 0.4 \times SGI, the SGI signal failed to increase, and even decreased a little, as shown in Fig. 2D and E. However, amplification of the template DNA was indeed completed, as verified by the electrophoresis results in Fig. 2F. This suggested that the negative results from the on-chip fluorescence were false-negative results. Increasing the SGI concentration from 0.4 \times to 1.6 \times helped to restore the vanished SGI signal, but the fluorescence increase was still insignificant, less than 100%.

Whatever factors should be blamed for SGI's poor performance on-chip, the CRoA enhancer helped to restore and enhance the SGI signal. With CRoA in the mixture, the droplets containing DNA templates brightened up normally after amplification at 0.4 \times SGI, with a 150% fluorescence increment, as shown in Fig. 2D–F. The fluorescence increment at higher SGI concentrations was also increased to a larger extent, ~200%. Fig. 2D also reveals that at the same SGI concentration, the fluorescence increase in the presence of CRoA was 3 times brighter than that without CRoA. CRoA functions in on-chip applications by utilizing a similar mechanism to off-chip. However, besides clipping and preventing SGI from interfering with the amplification process, in on-chip applications CRoA also acts as a shelter for SGI, protecting the dye molecules from factors that might hinder their function as amplification indicators.

As shown in Fig. 2E, the on-chip fluorescence images before amplification demonstrated the ability of CRoA to lower the background signal. Since the CRoA quencher moiety suppressed the intensity of the clipped dyes to a lower level than the free-floating dyes, the samples with CRoA looked darker than those without CRoA under the investigated fluorescence channel. The signal contrast before and after PCR was increased, and the fluorescence increase of the amplification was enhanced. This was consistent with the higher saturated fluorescence with CRoA than without CRoA in the off-chip amplification curves shown in Fig. 2A. Since the off-chip fluorescence shown here was a relative unit with baseline subtraction, the reduced background with CRoA resulted in a higher relative fluorescence signal at the plateau stage.

In Fig. 2F, a fade band above the product band showed up without CRoA, indicating nonspecific amplification. In the presence of CRoA, the product was much cleaner, with only the product band showing up. Nevertheless, samples with CRoA migrated faster than samples without CRoA. To test whether the presence of CRoA affected the specificity of PCR

amplification, the PCR products at $0.4\times$ SGI, both with CRoA and without CRoA, were sent out for Sanger sequencing. The perfectly matched sequencing results (Fig. S3†) indicated that CRoA had no negative effect on the amplification specificity. The offset of the band position on the gel image may be due to the complex interaction between the CRoA and the amplification product on the electrophoresis.

Optimization of CRoA function by stem length and concentration

To test the impact of the CRoA stem length on its function, we tested a series of CRoA termed “A n Q”, with n standing for the base pair number of the stem. To counteract the possible impact of the loop sequence on the function of CRoA, the loop was designed to consist of oligo A.

Fig. 3A and B show the comparative results of samples with these various CRoA enhancers at $0.4\times$ SGI, both on-chip and off-chip. For on-chip PCR, A0Q failed to function well, indicating that the stem in the hairpin structure of CRoA is a

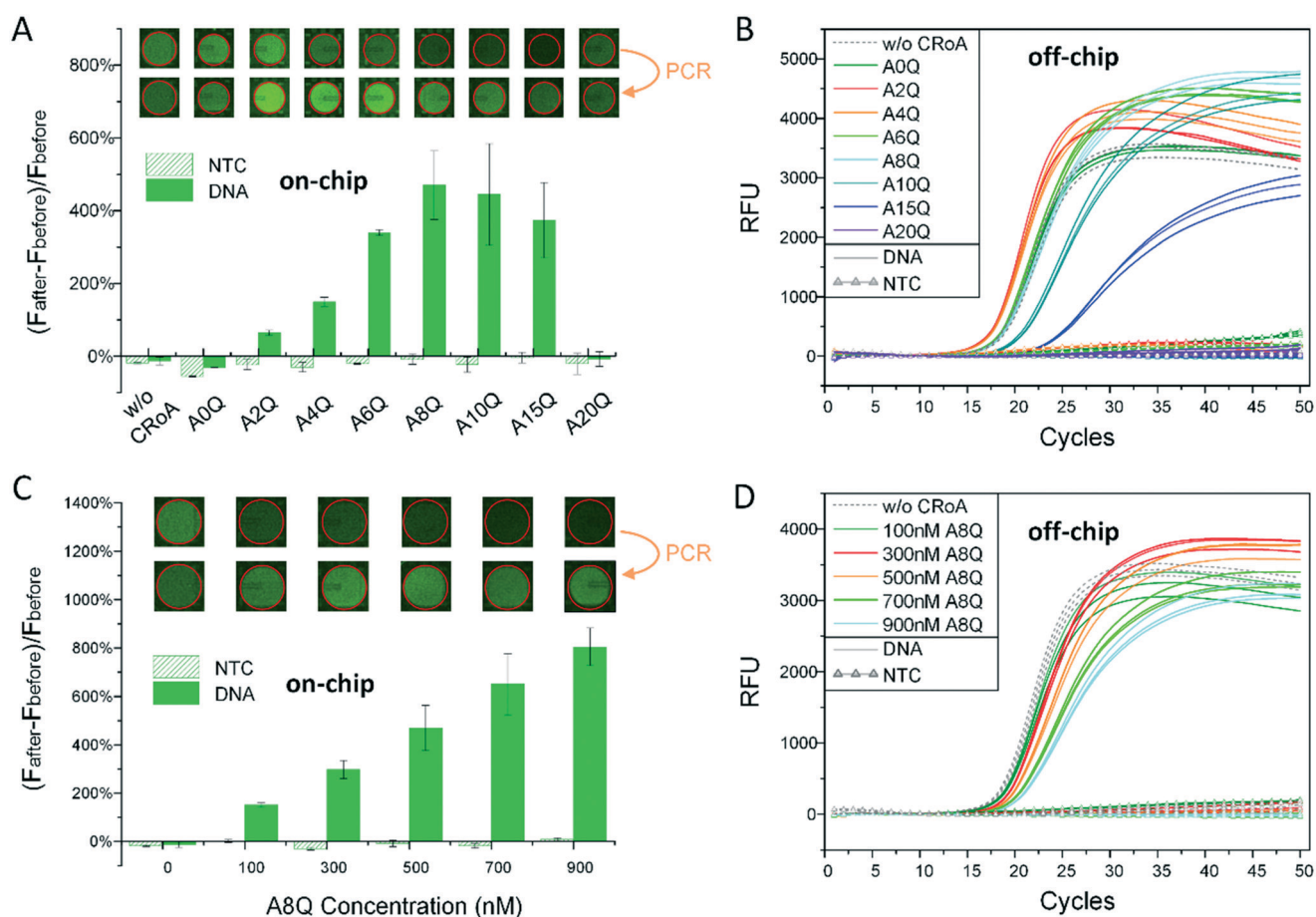


Fig. 3 The off-chip and on-chip PCR results for CRoA with various stem lengths and at various concentrations, at $0.4\times$ SGI. (A) End-point analysis results of on-chip PCR for samples with 500 nM CRoA, stem length ranging from 0 bp to 20 bp. Fluorescence images of one droplet in each triplicate of positive samples taken before and after PCR are also displayed. (B) Off-chip amplification curves for samples with 500 nM CRoA, stem length ranging from 0 bp to 20 bp. Controls w/o CRoA are also listed. (C) End-point analysis results of on-chip PCR for samples with 100–900 nM A8Q. Fluorescence images of one droplet in each triplicate of positive samples taken before and after PCR are also shown. (D) Off-chip amplification curves for samples with 100–900 nM A8Q. Controls w/o CRoA are also listed.

key motif. A20Q also caused failure in on-chip PCR, the same as the off-chip result. CRoA with stem length from 2 bp to 15 bp worked for on-chip PCR. Among them, A8Q performed the best on-chip, with a 500% fluorescence increment. Apparently, a longer stem offered more SGI binding sites, and its higher T_m rendered a larger fraction of CRoA to maintain its hairpin structure (evidence shown in Fig. S4†), leading to better performance. According to ref. 31, SGI's binding site on DNA is 3–4 bp, indicating an average binding of one SGI molecule per 3 to 4 bp of dsDNA. However, the interaction of SGI with DNA is complicated, with two binding modes: intercalation and minor groove binding. Which binding mode is prevalent highly depends on parameters such as salts, solution viscosity and dye/DNA ratio.^{12,32} Based on Fig. 3A and B, a 2 bp stem can trap at least one dye molecule. What's more, the fluorescence of the droplets before PCR in Fig. 3A revealed a trend in decreasing background fluorescence before amplification as the hairpin stem was extended from 2 bp to 15 bp, while the 20 bp stem caused a sudden increase in the background fluorescence. This indicated an enhanced overall quenching effect as the stem became longer in the range of 2 bp to 15 bp. However, with stems longer than 8 bp, the inhibition of amplification

by CRoA, as shown in Fig. 3B, counteracted the bright side of CRoA and cut down the fluorescence increment. In the off-chip assay, A10Q led to a delay in the C_q value for 2 cycles and A15Q for 10 cycles. Further increasing the CRoA stem length to 20 bp resulted in amplification failure.

Then, using A8Q as a model, the impact of CRoA concentration on its enhancement efficiency was tested. For on-chip PCR, as revealed by Fig. 3C, the higher the concentration of A8Q, the better the PCR performance. An on-chip fluorescence increment as large as 800% was gained by samples with 900 nM A8Q at 0.4× SGI. On the other hand, in the off-chip assay, as shown in Fig. 3D, increasing the CRoA concentration from 100 nM to 900 nM showed some inhibition of PCR at 0.4× SGI, but to a trivial extent.

Impact of quencher and loop on CRoA function

The structure of CRoA can be simply divided into a hairpin consisting of a loop sequence and a stem, plus a quencher moiety attached to the 3' end. The performance of A0Q shown in Fig. 3B indicates the importance of the double-stranded stem. To test the effect of the quencher moiety and loop specificity, we adjusted the structure of A4Q (Fig. 4A) to

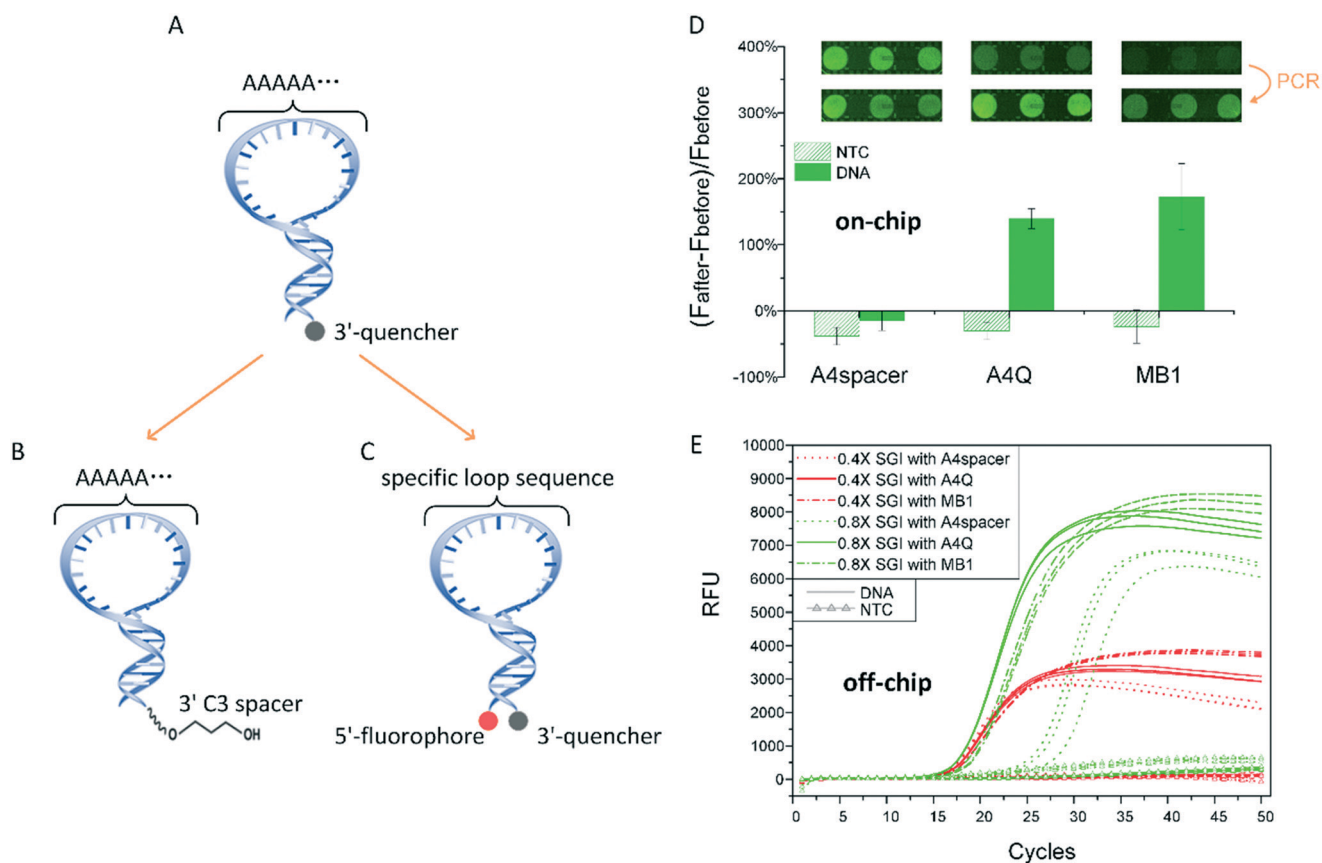


Fig. 4 Structural change from A4Q to A4spacer and the MB probe and their function in off-chip and on-chip PCR. (A) Schematic of A4Q. (B) Schematic of A4spacer, with a C3 spacer modified at the 3' end. (C) Schematic of the MB probe, with a loop sequence specific to the target. (D) End-point analysis results of on-chip PCR for samples with A4spacer, A4Q, and MB1, respectively, at 0.4× SGI. Fluorescence images of positive samples taken before and after PCR are also shown. (E) Off-chip amplification curves for samples with A4spacer, A4Q, and MB1, respectively, at 0.4× and 0.8× SGI.

A4spacer (Fig. 4B) and MB1 (Fig. 4C), and applied these in the above PCR system, respectively.

As shown in Fig. 4D and E, A4spacer failed to enhance both on-chip and off-chip PCR, while MB1 still worked. For on-chip PCR at 0.4× SGI, Fig. 4D shows that samples with A4spacer did not brighten after amplification, and the signal of some droplets even decreased. On the other hand, MB1 succeeded in restoring the SGI signal after on-chip amplification, with a fluorescence increase of nearly 200%. It is also worth noting that in the presence of MB1, the signal before PCR was lower than that for the samples with A4Q. This may be attributed to the 5' CY5 fluorophore of MB1, the absorption spectrum of which overlaps with SGI's emission spectrum. The 5' fluorophore of MB1 can thus absorb part of the SGI signal, rendering a lower background. For off-chip PCR at 0.4× SGI, the three groups of samples showed no difference in the C_q value. However, at 0.8× SGI, MB1 canceled out the dye-mediated PCR inhibition, just like A4Q, while the samples with A4spacer had a delayed C_q for 5 cycles.

Thus, we conclude that a 3' moiety in CRoA to turn off the signal of the clipped dye is necessary for the enhancer's function. Therefore any moiety that can absorb the emission fluorescence of the clipped dye, including but not limited to the generally used quenchers, should work as well. On the

other hand, the loop sequence is a trivial factor. However, a nonspecific loop sequence is preferable to avoid interference with amplification resulting from the loop's hybridization with templates.

Dynamic range of SGI and impact of CRoA on amplification sensitivity and specificity

From the above results, we discovered that more SGI could be added to the PCR mixture in the presence of CRoA, which gave a higher end-point fluorescence signal. To explore the upper limit of SGI concentration that can be applied in PCR, we screened a series of A8Q concentrations at different SGI levels from 0.8× to 2.0×.

Fig. 5A shows off-chip amplification results at each SGI level. The A8Q concentration listed in Fig. 5A was the minimum amount of A8Q required at each SGI level for best performance. The amplification curves of the samples at 0.2× SGI and 0.4× SGI without CRoA are also listed as control groups. Through this optimization of A8Q concentration, as much as 1.2× SGI was used in PCR without causing any inhibition, and nearly 8 times greater fluorescence was gained than at 0.2× SGI. At 1.6× SGI and 2.0× SGI, the fluorescence change further increased, although with a reduced

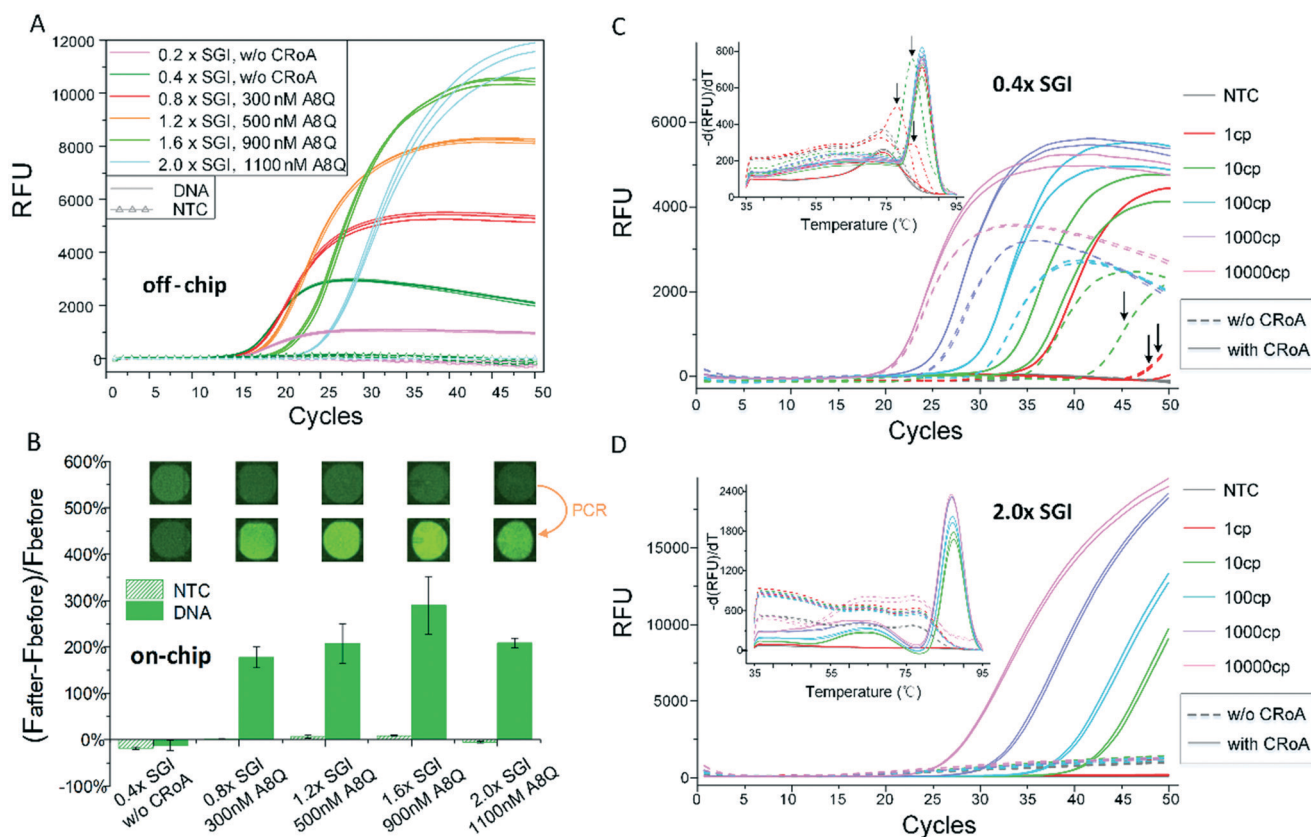


Fig. 5 The optimized off-chip amplification results (A) and their on-chip performance (B) at different SGI levels. A8Q concentrations listed here are the lowest A8Q concentrations needed to gain the greatest PCR enhancement at each SGI level. (C) Off-chip amplification of human genomic DNA, from 1 cp to 1×10^4 cp, for samples w/o CRoA and samples with 500 nM A4Q, at 0.4× SGI. The arrows indicate nonspecific products. (D) Off-chip amplification of human genomic DNA, from 1 cp to 1×10^4 cp, for samples w/o CRoA and samples with 1100 nM A8Q, at 2.0× SGI.

amplification efficiency, and the saturated fluorescence was boosted up to 10-fold. We thus conclude that CRoA greatly broadens the dynamic range of SGI's usage, and generates higher fluorescence reported by SGI in amplification.

On-chip PCR trials for the corresponding samples were also conducted, and the results are shown in Fig. 5B. With CRoA, the fluorescence increment after amplification doubled when the SGI concentration increased from 0.8× to 1.6×, while a further increase to 2.0× caused a decrease in fluorescence. This might be explained by the reduced amplification efficiency at 2.0× SGI, indicated by the delayed C_q for 10 cycles in off-chip PCR. At the cutoff time for end-point analysis, the amplification may have not reached a plateau yet.

Additionally, the amplification sensitivity and specificity with CRoA were tested at 0.4× and 2.0× SGI, respectively. Ten-fold serial diluted human genomic DNA was used as a template, from 3.5 pg to 35 ng (from 1 cp to 1×10^4 cp). As shown in Fig. 5C, at 0.4× SGI, as little as 10 cp of the starting template could be amplified without CRoA. Adding 500 nM A4Q to the reaction mixture increased the detection limit to 1 cp. Moreover, CRoA eliminated the nonspecific amplification products in cases of low abundance templates when CRoA was absent, as determined by the melting peak. At 2.0× SGI, as displayed in Fig. 5D, the amplification of templates at all dilutions failed without CRoA. By adding 1100 nM A8Q, as previously optimized, the amplification sensitivity was increased to a large extent, with the limit of detection being 10 cp. Besides, the presence of CRoA not only increased the detection sensitivity, but also cleaned up nonspecific amplifications in all cases. The underlying mechanism for this improved specificity by CRoA is not thoroughly explored in this work. However, it is possible that the presence of CRoA can reduce the dyes' binding with the primer-target complex, thus reducing the primer's T_m with its target, since dsDNA-binding dyes have been reported to be able to stabilize duplex DNA.³³ As shown in Fig. S5,† the primer's T_m with a mutant target was affected more than that with the completely complementary target, although both were decreased by CRoA. Since the annealing temperature of PCR remained unchanged, adding CRoA might lower the T_m of the mispriming complex to a level that blocks nonspecific amplification, thus increasing specificity.

General application of CRoA for enhancing DNA amplification

So far, the enhancing function of CRoA in PCR systems using SGI has been proven in principle by amplification of the G269 target. To verify that CRoA can act as a more general DNA amplification enhancer, we tested its application with various dsDNA-binding dyes on various DNA targets, using various DNA amplification methods and on various microfluidic platforms.

To verify whether the clip-to-release on amplification mechanism works for other dsDNA-binding dyes, we tested the performance of CRoA in PCR systems using Sytox Green or EvaGreen as dsDNA-binding dyes, respectively. Sytox Green

and EvaGreen share similar excitation/emission spectra to SGI, so their fluorescence signals can be quenched by the same quencher as used above.

As revealed in Fig. 6A, the addition of CRoA doubled the fluorescence signal of positive samples in the on-chip PCR assay when 200 nM Sytox Green was applied as the amplification indicator. For the off-chip assay, as revealed in Fig. 6B, similarly to SGI, Sytox Green showed inhibition of amplification at a concentration of 400 nM and terminated PCR at 500 nM in the absence of CRoA. With CRoA, 400 nM of Sytox Green had no negative effect on the PCR efficiency, while 500 nM delayed PCR but still resulted in successful amplification.

For EvaGreen, CRoA also made a great improvement to the dye signal in on-chip nucleic acid amplification. As Fig. 6C reveals, the addition of CRoA boosted the end-point amplification signal of on-chip PCR at 1× EvaGreen by almost two-fold. The background fluorescence signal before amplification was lowered to a significant extent so that the signal contrast of the positive samples before and after amplification was obviously improved. On the other hand, in off-chip assays, the addition of CRoA did not make a difference to the amplification efficiency when EvaGreen was used, in contrast to the significant enhancing effect observed with SGI and Sytox Green as the indicators. Due to EvaGreen's homodimeric configuration and its ability to shift between the "inactive" form (bent form) and the "active" form (linear form),^{34,35} this dye can generate active dyes on demand as PCR proceeds. In this case, as revealed in Fig. 6D, EvaGreen itself showed little inhibition of PCR at the commonly used 1× or 2× concentration,⁵ offering CRoA no opportunity to display its enhancing ability off-chip. Although EvaGreen shared a similar concept of "release on demand" to dsDNA-binding dyes, it was realized by conformational change in an environment-dependent manner.^{35,36} In the CRoA strategy, the dyes underwent positional change from a shorter dsDNA region to a longer dsDNA region in a less environment-dependent manner. These two strategies functioned complementarily, not in conflict with each other. Thus, CRoA could still work for EvaGreen, especially in on-chip applications where CRoA might offer protection for the dye molecules. Moreover, improved amplification sensitivity and specificity were observed in off-chip PCR assays using EvaGreen, as revealed in Fig. S6 in the ESI.†

Based on these results, we verified that CRoA also works for other dsDNA-binding dyes, especially in on-chip applications. For EvaGreen, CRoA increases the dye signal as an amplification indicator for on-chip PCR. For other dyes, such as SGI and Sytox Green, CRoA can not only enhance the fluorescence signal of on-chip amplification, but also reduce dye-mediated PCR inhibition at high concentrations of the dyes.

To prove the efficacy of CRoA in different DNA amplification systems for various targets, we applied CRoA in two other nucleic acid amplification systems: a PCR assay for the human *KRAS* gene and a LAMP assay to detect the *T. brucei* *SRA* gene. In both assays, SGI was applied at different

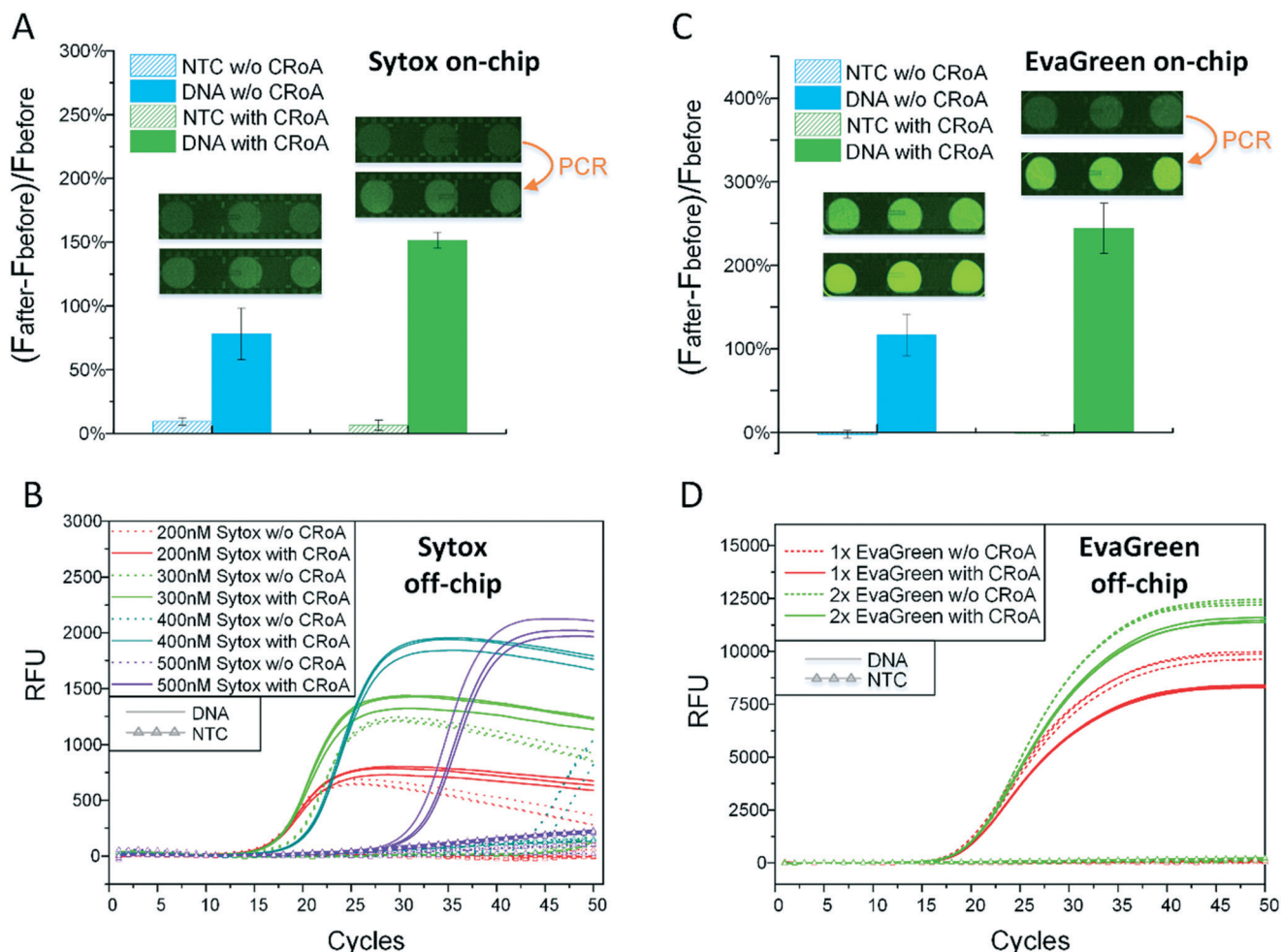


Fig. 6 CRoA PCR enhancing function in reactions utilizing other dsDNA-binding dyes. (A) End-point analysis results of on-chip PCR for samples w/o CRoA and with 500 nM A4Q, at 200 nM Sytox Green. (B) Off-chip amplification curves and comparison between samples w/o CRoA and with 500 nM A4Q at various Sytox Green concentrations. (C) End-point analysis results of on-chip PCR for samples w/o CRoA and with 1 μ M A8Q, at 1 \times EvaGreen. (D) Off-chip amplification curves and comparison between samples w/o CRoA and with 1 μ M A8Q at 1 \times and 2 \times EvaGreen.

levels, together with the above optimized concentration of A8Q. Samples without CRoA were also run as control groups.

As Fig. 7A shows, CRoA functioned well in the *KRAS* PCR system. Without CRoA, 0.8 \times SGI induced an obvious delay in the C_q value, and 1.2 \times SGI caused the amplification to fail. With CRoA, increasing the SGI concentration from 0.4 \times SGI to 1.2 \times did not cause any inhibition of amplification. Additionally, we also demonstrated the function of CRoA to enhance amplification in nucleic acid amplification systems besides PCR in the *T. brucei* LAMP assay, as Fig. 7B reveals. This LAMP assay was more tolerant of higher levels of SGI in the absence of CRoA: 0.8 \times SGI led to about 3 minutes of delay, and 1.2 \times SGI led to about 10 minutes of delay. However, adding CRoA undoubtedly benefited the LAMP reaction. With the addition of the optimized concentration of A8Q, 1.2 \times SGI only induced 1 minute of delay, indicating minor inhibition in the presence of CRoA.

To verify the general application of CRoA on microfluidic platforms other than digital microfluidics, we also performed G269 asymmetric PCR on a polydimethylsiloxane (PDMS) based

channel microfluidic system. A schematic of the PDMS chip is shown in Fig. 8A and B. Detailed fabrication and operation processes can be found in the ESI.† The molecular beacon probe (MB2) applied to determine amplicon specificity also worked as a CRoA enhancer, as already discussed.

As Fig. 8C shows, the signal of the molecular beacon probe under the CY3 channel indicated successful and specific amplification. However, for samples without CRoA (MB2 here), even though SGI at a low concentration (0.24 \times) was used here, its background fluorescence under the GFP channel was bright before amplification. In contrast to the amplification result, the SGI signal decreased to nearly nothing after PCR. By adding the CRoA enhancer to the reaction mixture, this unexpected phenomenon disappeared. For samples with both SGI and CRoA, SGI restored its function as an amplification indicator, with a low background signal before amplification and an elevated signal after PCR. This was highly consistent with what we observed on digital microfluidic chips: CRoA reduced the SGI background signal before amplification and increased its

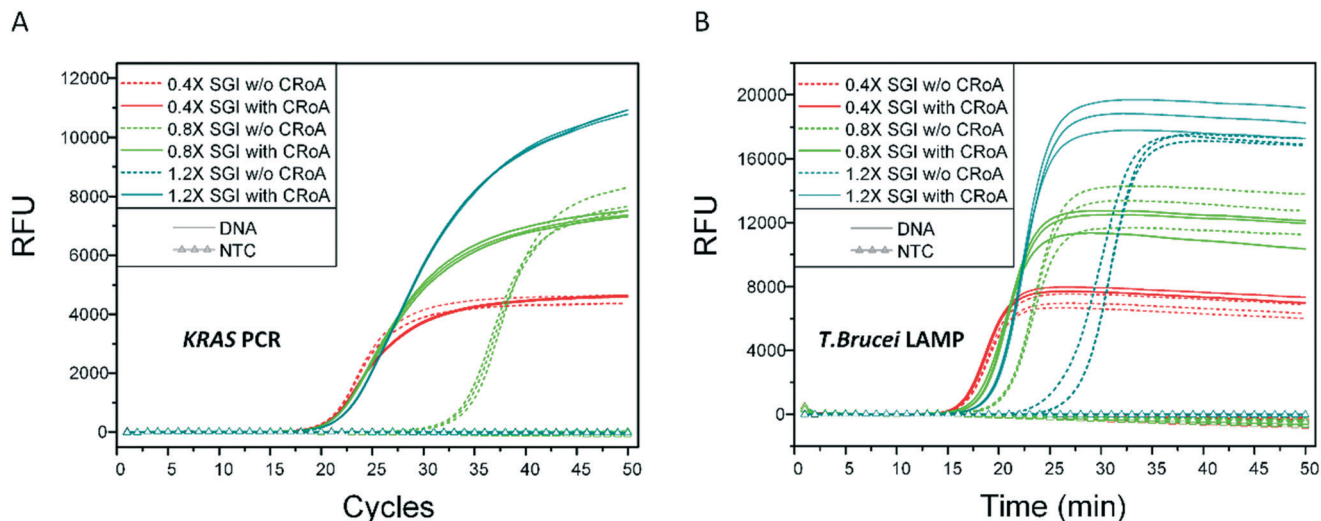


Fig. 7 CRoA PCR enhancing performance in other nucleic acid amplification systems. CRoA was applied with different concentrations at different SGI levels: 100 nM of A8Q at 0.4 \times SGI, 300 nM of A8Q at 0.8 \times SGI, and 500 nM of A8Q at 1.2 \times SGI. Samples without CRoA were run as controls. (A) Off-chip amplification curves in the *KRAS* PCR assay. (B) Off-chip amplification curves in the *T. brucei* LAMP assay.

signal after amplification, thus improving the fluorescence contrast.

Based on the above results, we conclude that CRoA as an on-chip PCR enhancer is not restricted to the DMF system, but works generally for microfluidic platforms.

As a brief summary, CRoA works universally to promote the amplification of different targets in different nucleic acid amplification systems, as long as dsDNA-binding dyes are employed. With the general utilization of CRoA, we can

foresee the utilization of dsDNA dyes for nucleic acid amplification in a broader and more robust way.

Conclusions

In this study, we propose a novel DNA amplification enhancer named CRoA to promote amplification in the presence of dsDNA-binding dyes. CRoA benefits amplification by acting as a temporary reservoir for the dsDNA-binding dyes and

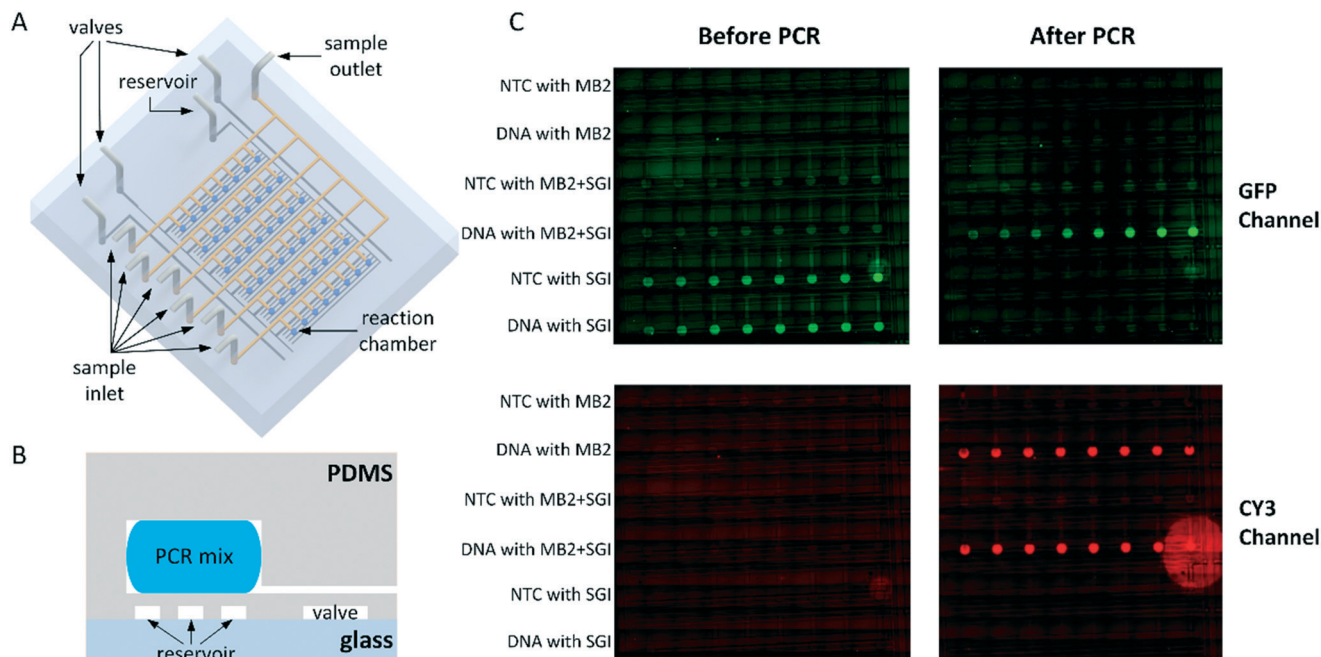


Fig. 8 CRoA as an on-chip PCR enhancer on a PDMS-based channel microfluidic chip. (A and B) Top view and side view schematic of the PDMS channel microfluidic chip. (C) Fluorescence microscopy images under GFP and CY3 channels of the on-chip PCR chambers, before and after amplification.

modulating the number of dye molecules in the solution. By adjusting the number of free-floating dye molecules, CRoA can reduce the inhibitory effect of a high concentration of dye on the amplification efficiency. The experimental results showed a significant amplification enhancement. With the integration of the proposed enhancer, higher levels of dsDNA-binding dyes can be applied without causing inhibition, and the fluorescence signal of the dye was boosted up to 10-fold after amplification. Moreover, an additional effect of CRoA in increasing amplification specificity, especially for low abundance templates, was suggested.

In on-chip applications, CRoA functions in the same temporary storage and release on-demand manner, but with an extra beneficial effect. By providing binding sites for the dsDNA-binding dye, the proposed CRoA is capable of sheltering the dye from on-chip damaging factors. In both the digital microfluidic chip and the PDMS-based channel microfluidic chip, adding CRoA to the reaction mixture restored the fluorescence signal of the false-negative results.

PCR enhancers targeting dsDNA-binding dyes have been proposed and investigated before, as already discussed in the introduction.^{24,28,29} However, the enhancing effect of most of these existing enhancers could only be modulated by changing the concentrations of additives, thus in a restricted manner. In contrast, CRoA functions through attraction of the stem to the dsDNA-binding dye, which is ion independent, and its performance can be modulated not only by concentration, but also *via* fine tuning of different motifs of the CRoA structure, in a more flexible manner. Among the three parts of the CRoA structure, the stem and the 3' quencher are key components, while the loop sequence matters little.

The robustness and broad utility of CRoA as a DNA amplification enhancer for both on-chip and off-chip applications has been demonstrated. Besides, the finding that CRoA enables the utilization of SGI at a high concentration offers the possibility that SGI may find applications in areas such as high resolution melting (HRM) analysis. SGI has never been considered as a possible HRM dye because its PCR inhibition effect limits the use of the dye to a low concentration range, resulting in insufficient sensitivity for HRM. However, with CRoA, SGI can be used at higher concentrations, offering an elevated signal and higher resolution for HRM.

The clip-to-release on amplification mechanism that CRoA utilizes to enhance PCR is simple but effective. With the help of CRoA, the drawbacks of dsDNA-binding dyes can be mitigated, enabling the more flexible and robust utilization of nucleic acid amplification methods in both off-chip and on-chip scenarios.

A patent has been filed.

Author contributions

Conceptualization, R. S. and Y. J.; methodology, R. S. and Y. J.; investigation, R. S. and Y. J.; formal analysis, R. S. and Y. J.; writing – original draft, R. S.; writing – review and editing, Y. J., P. M. and R. P. M.; supervision, Y. J., P. M. and R. P. M.; funding acquisition, Y. J., P. M. and R. P. M.

Conflicts of interest

The authors declare no competing interests.

Acknowledgements

This work was supported by Macau Science and Technology Development Fund (FDCT) [FDCT110/2016/A3, FDCT 0053/2019/A1, AMSV SKL Fund]; University of Macau [MYRG2017-00022-AMSV, MYRG2018-00114-AMSV]; and DAAN Gene Co., Ltd. [EF009/AMSV-JYW/2018/GSTIC].

We are grateful to Prof. Lawrence Wangh from ThermaGenix Inc. for valuable discussions and helpful suggestions. We would also like to thank the technical and administrative team of the State Key Laboratory of Analog and Mixed-Signal VLSI at University of Macau for all their support.

References

- 1 E. Navarro, G. Serrano-Heras, M. J. Castano and J. Solera, *Clin. Chim. Acta*, 2015, **439**, 231–250.
- 2 S. J. Smith, C. R. Nembr and S. O. Kelley, *J. Am. Chem. Soc.*, 2017, **139**, 1020–1028.
- 3 R. Higuchi, C. Fockler, G. Dollinger and R. Watson, *Bio/Technology*, 1993, **11**, 1026–1030.
- 4 K. M. Ririe, R. P. Rasmussen and C. T. Wittwer, *Anal. Biochem.*, 1997, **245**, 154–160.
- 5 F. Mao, W. Y. Leung and X. Xin, *BMC Biotechnol.*, 2007, **7**, 76.
- 6 P. Lebaron, P. Catala and N. Parthuisot, *Appl. Environ. Microbiol.*, 1998, **64**, 2697–2700.
- 7 P. M. Holland, R. D. Abramson, R. Watson and D. H. Gelfand, *Proc. Natl. Acad. Sci. U. S. A.*, 1991, **88**, 7276–7280.
- 8 C. A. Heid, J. Stevens, K. J. Livak and P. M. Williams, *Genome Res.*, 1996, **6**, 986–994.
- 9 S. Tyagi and F. R. Kramer, *Nat. Biotechnol.*, 1996, **14**, 303–308.
- 10 J. A. Vet and S. A. Marras, *Methods Mol. Biol.*, 2005, **288**, 273–290.
- 11 H. Gudnason, M. Dufva, D. D. Bang and A. Wolff, *Nucleic Acids Res.*, 2007, **35**, e127.
- 12 H. Zipper, H. Brunner, J. Bernhagen and F. Vitzthum, *Nucleic Acids Res.*, 2004, **32**, e103.
- 13 A. L. Benveniste, Y. Creeger, G. W. Fisher, B. Ballou, A. S. Waggoner and B. A. Armitage, *J. Am. Chem. Soc.*, 2007, **129**, 2025–2034.
- 14 A. S. Biebricher, I. Heller, R. F. Roijmans, T. P. Hoekstra, E. J. Peterman and G. J. Wuite, *Nat. Commun.*, 2015, **6**, 7304.
- 15 C. Zhang and D. Xing, *Nucleic Acids Res.*, 2007, **35**, 4223–4237.
- 16 C. D. Ahrberg, A. Manz and B. G. Chung, *Lab Chip*, 2016, **16**, 3866–3884.
- 17 B. Coelho, B. Veigas, E. Fortunato, R. Martins, H. Águas, R. Igreja and P. V. Baptista, *Sensors*, 2017, **17**, 1495.
- 18 T. Houssin, J. Cramer, R. Grojsman, L. Bellahsene, G. Colas, H. Moulet, W. Minnella, C. Pannetier, M. Leberre, A. Plecis and Y. Chen, *Lab Chip*, 2016, **16**, 1401–1411.
- 19 Y. Fu, X. Zhou and D. Xing, *Lab Chip*, 2017, **17**, 4334–4341.

- 20 A. Hassibi, A. Manickam, R. Singh, S. Bolouki, R. Sinha, K. B. Jirage, M. W. McDermott, B. Hassibi, H. Vikalo, G. Mazarei, L. Pei, L. Bousse, M. Miller, M. Heshami, M. P. Savage, M. T. Taylor, N. Gamini, N. Wood, P. Mantina, P. Grogan, P. Kuimelis, P. Savalia, S. Conradson, Y. Li, R. B. Meyer, E. Ku, J. Ebert, B. A. Pinsky, G. Dolganov, T. Van, K. A. Johnson, P. Naraghi-Arani, R. G. Kuimelis and G. Schoolnik, *Nat. Biotechnol.*, 2018, **36**, 738.
- 21 K. M. Shen, N. M. Sabbavarapu, C. Y. Fu, J. T. Jan, J. R. Wang, S. C. Hung and G. B. Lee, *Lab Chip*, 2019, **19**, 1277–1286.
- 22 S. Feng, S. Mao, J. Dou, W. Li, H. Li and J.-M. Lin, *Chem. Sci.*, 2019, **10**, 8571–8576.
- 23 J. Yin, Z. Zou, Z. Hu, S. Zhang, F. Zhang, B. Wang, S. LV and Y. Mu, *Lab Chip*, 2020, **20**, 979–986.
- 24 J. E. Kong, Q. Wei, D. Tseng, J. Zhang, E. Pan, M. Lewinski, O. B. Garner, A. Ozcan and D. Di Carlo, *ACS Nano*, 2017, **11**, 2934–2943.
- 25 T. Wu, H. Suzuki, Y. Su, Z. Tang, L. Zhang and T. Yomo, *Soft Matter*, 2013, **9**, 3473–3477.
- 26 C. Kanony, B. Åkerman and E. Tuite, *J. Am. Chem. Soc.*, 2001, **123**, 7985–7995.
- 27 J. H. van der Velde, J. Oelerich, J. Huang, J. H. Smit, A. Aminian Jazi, S. Galiani, K. Kolmakov, G. Guoridis, C. Eggeling, A. Herrmann, G. Roelfes and T. Cordes, *Nat. Commun.*, 2016, **7**, 10144.
- 28 G. M. Shaik, L. Dráberová, P. Dráber, M. Boubelík and P. Dráber, *Nucleic Acids Res.*, 2008, **36**, e93–e93.
- 29 K. Nath, J. W. Sarosy, J. Hahn and C. J. Di Como, *J. Biochem. Biophys. Methods*, 2000, **42**, 15–29.
- 30 S. Giglio, P. T. Monis and C. P. Saint, *Nucleic Acids Res.*, 2003, **31**, e136–e136.
- 31 A. I. Dragan, R. Pavlovic, J. B. McGivney, J. R. Casas-Finet, E. S. Bishop, R. J. Strouse, M. A. Schenerman and C. D. Geddes, *J. Fluoresc.*, 2012, **22**, 1189–1199.
- 32 B. A. Armitage, *DNA Binders and Related Subjects*, 2005, pp. 55–76, DOI: 10.1007/b100442.
- 33 Y. Ke, G. Bellot, N. V. Voigt, E. Fradkov and W. M. Shih, *Chem. Sci.*, 2012, **3**, 2587–2597.
- 34 S. L. McIntosh, T. G. Deligeorgiev, N. I. Gadjev and L. B. McGown, *Electrophoresis*, 2002, **23**, 1473–1479.
- 35 L. Shoute and G. Loppnow, *Phys. Chem. Chem. Phys.*, 2018, **20**, 4772–4780.
- 36 B. H. Robinson, A. Löffler and G. Schwarz, *J. Chem. Soc., Faraday Trans. 1*, 1973, **69**, 56–69.